VAREHD 12th Conference on EHD
Lubrication and Traction, October 8-9 2004,
Suceava, Romania

AN ANALYTICAL AND NUMERICAL APPROACH OF LOAD CARRYING CAPACITY FOR PARTIALLY TEXTURED SLIDERS

Mircea PASCOVICI, Victor MARIAN - *Department of Machine Elements and Tribology,*
University Politehnica of Bucharest – Bucharest , Romania,
mircea@meca.omtr.pub.ro

ABSTRACT

Partially textured sliders generate a load carrying capacity with an effect similar to stepped bearings. The present paper presents a theoretical investigation of a partially textured slider using an analytical and numerical method. The pressure distribution is calculated analytically and numerically and the performance of the bearing is evaluated varying different parameters: number of dimples, dimple density, dimple height, textured fraction of the slider. The optimal configuration for the slider is determined in order to produce maximal load carrying capacity.

1. NOMENCLATURE

a	"active" length of textured zone
b	length of untextured zone
h	film thickness
$H = \frac{h_m + s}{h_m}$	dimensionless film thickness
h_m	minimum film thickness
ℓ	dimple side length
L	cell side length
L_t	textured length
L_{tot}	total length of the slider
N	number of dimples on one row
p	manometric pressure
$\overline{p} = \frac{p \cdot h_m^{\,2}}{\eta \cdot U \cdot L_{tot}}$	dimensionless pressure
s	dimple depth

U	sliding velocity
x	longitudinal axis of the slider
z	lateral axis of the slider
$\alpha = L_t / L_{tot}$	textured fraction
β	dimensionless untextured length, b/L
η	liquid viscosity
$\Lambda=(L-\ell)/L$	dimensionless length of sills
$\rho=(\ell/L)^2$	texture density

2. INTRODUCTION

The idea of surface texturing began in 1965 when a load carrying capacity between parallel surfaces was observed in the case of mechanical seals [8].

The concept was developed after 1990 with the development of the laser technology. Surface texturing found a large number of industrial applications. In the case of mechanical seals this technology enhanced the axial stiffness of mechanical seals [2-4,6]. By texturing the piston rings or the cylinder liner the friction force can be diminished by up to 30% in the case of internal combustion engines [7,9,10].

Axial thrust bearings were manufactured by partially texturing the surface of stator by laser surface texturing. In this case the dimples have a spherical form. The pressure distribution of these bearings was theoretically and experimentally investigated [1,5].

In the present paper a partially textured slider having dimples of square form is investigated. The slider can be textured by lithography, the advantage of this technique consisting on the rapidity in texturing the surface.

3. ANALYSIS

For the sake of simplicity the slider is considered infinitely wide. So only one row can be considered with zero flow on the sides (Figure 1). The pressure at the inlet and outlet of the slider is considered to be zero (atmospheric pressure).

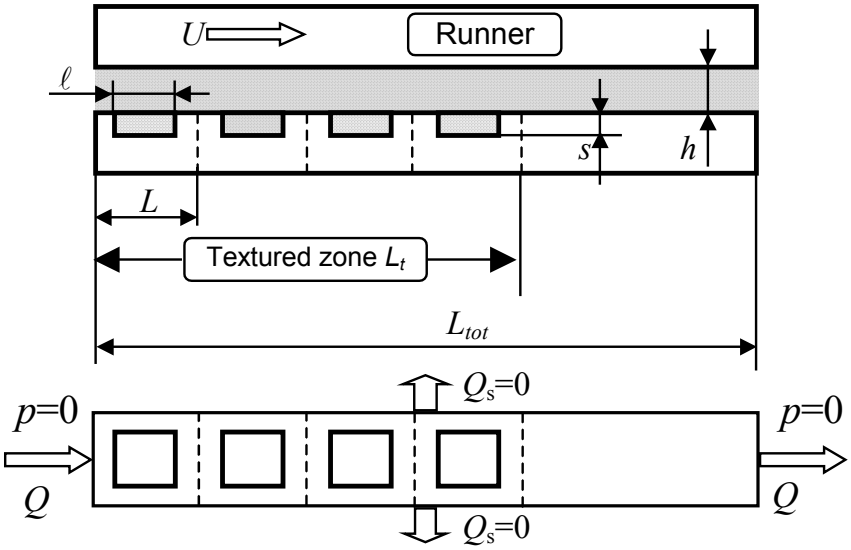

Figure1: simplified model

4. ANALYTICAL MODEL

The following main assumptions are accepted:
- the fluid film is a Newtonian liquid in laminar and isothermal flow ;
- only one row is considered with zero flow on the sides
- the pressure distribution on the longitudinal direction is linear
- all the current assumptions for thin film lubricant are also accepted

The geometry of the model and the assumed pressure distribution is presented in Figure 2. If the textured zone starts with a sill, then the pressure gradient must be negative on the starting sill from reason of longitudinal rate of flow (Q_x) conservation. In other words the Poisseuille rate of flow must introduce lubricant in the first cell. In this way implicitly the appearance of depression (cavitation) is considered. This depression is quantified by the pressure p_c. But the p_c pressure is relatively small in comparison with the other pressure components (p_b, p_i, p_m, p_{mov}, see Fig.2) and for reasons of computation simplification the pressured distribution with interrupted line will be considered. This pressure distribution is similar with that one encountered for spiral groove thrust bearings. In this case the first sill (the OO' segment in Fig.2), the pressure will be considered zero, assumption used for the divergent zone in other lubrication problems as journal bearings. The results obtained under this approximation could be rectified subsequently identifying the p_c pressure and obtaining the "real" pressure distribution drawn with continuous line in Fig.2.

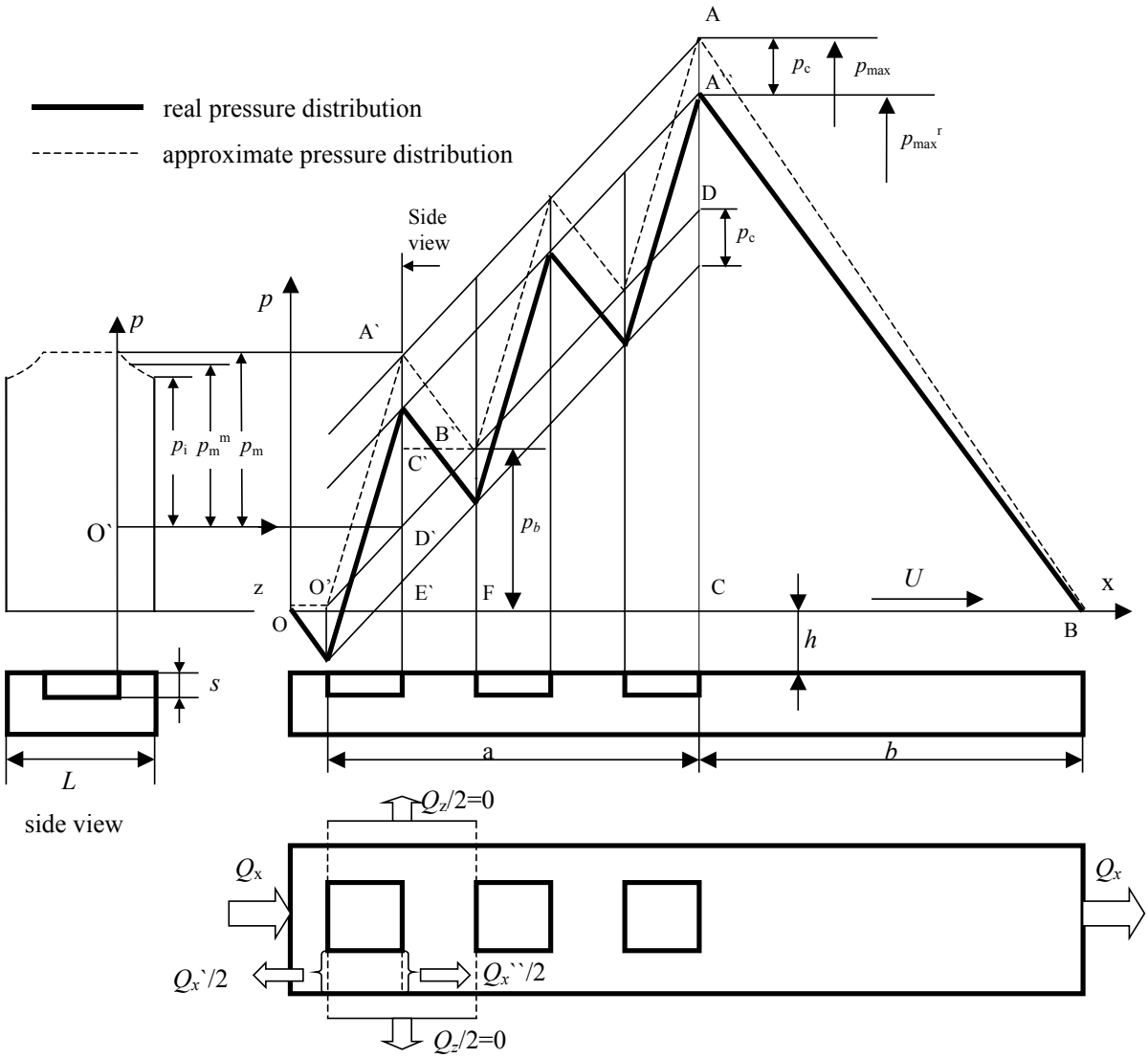

Figure 2

Using the pressure distribution drawn in Figure 2 we obtain geometrically the following relationships between the pressure components:

From the similitude of the triangles ΔO`CD ~ ΔO`B`F

$$p_b = \frac{p_{\max} - p_m}{N - \Lambda} \tag{1}$$

From similitude of triangles ΔABC ~ ΔA`B`C`

$$p_{\max} = \frac{\beta}{\Lambda}(p_m - \Lambda \cdot p_b) \tag{2}$$

From relationships (1) and (2) we have:

$$p_{\max} = p_m \frac{\beta \cdot N}{\Lambda(N + \beta - \lambda)} \tag{3}$$

and

$$p_b = p_m \cdot \frac{(\beta - \Lambda)}{\Lambda \cdot (N + \beta - \Lambda)} \tag{4}$$

A virtual flow rate balance at the cell level in the local maximum pressure area will be considered for taking in consideration the recirculation flow:

$$Q_z/2 = Q`_x/2 + Q``_x/2 \tag{5}$$

Assuming that the pressure distribution in the z direction is parabolic and satisfying the condition of zero side flow at the boundary between the two rows it results:

$$\left.\frac{dp}{dz}\right|_{z=0}^{m,} = -\frac{2(p_m - p_i)}{L - \ell} \tag{6}$$

Between the mean pressure p_m^m and the end values p_m and p_i of parabolic pressure distribution we have

$$p_i = \frac{3p_m^m - p_m}{2} \tag{7}$$

Finally we obtain the key relationship between mean and maximum local pressures, see Fig.2 :

$$p_m^m = p_m \frac{6(1 - \Lambda)}{6 - 5\Lambda} \tag{8}$$

The balance of Couette and Poisseuille flow rates gives:

$$\frac{\ell \cdot U \cdot s}{2} = \frac{\ell \cdot (h+s)^3 (p_m + (1-\Lambda)p_b)}{12 \cdot \eta \cdot \ell} + \frac{\ell \cdot h^3 (p_m - \Lambda \cdot p_b)}{12 \cdot \eta \cdot (L - \ell)} + \frac{(L-\ell) \cdot h^3}{12 \cdot \eta} \left[\frac{p_m^m + (1-\Lambda)p_b}{\ell} + \frac{p_m^m - \Lambda \cdot p_b}{L - \ell} \right] \tag{9}$$

Taking into consideration equations (4) and (8) we have:

$$\overline{p_m} = \frac{p_m \cdot h^2}{\eta \cdot U \cdot L} = \frac{6(H-1)(1-\Lambda)}{\frac{H^3(\Lambda N + \beta - \Lambda) + N(1-\Lambda)}{\Lambda(N + \beta - \Lambda)} + \frac{6}{6 - 5\Lambda}} \tag{10}$$

Using the relationship (3) we obtain the expression of the dimensionless maximum pressure, a key parameter of the load carrying capacity problem:

$$\overline{p}_{\max} = \frac{p_{\max} \cdot h^2}{\eta \cdot U \cdot L_{tot}} = \frac{6\beta N(H-1)(1-\Lambda)}{[H^3(\Lambda N + \beta - \Lambda) + N(1-\Lambda) + \frac{6\Lambda(N + \beta - \Lambda)}{6 - 5\Lambda}](N + \beta - 0.5\Lambda)} \tag{11}$$

The correction necessary to reach the maximum pressure $p_{\max}^r$ is found from the similitude between the triangle ΔOO`G ~ ΔA``BC

$$p_c = p_{\max}^r \frac{\Lambda}{2\beta} \tag{12}$$

but (see Fig.2)

$$p_{\max} = p_{\max}^r + p_c \tag{13}$$

then

$$p^{r}_{\max} = p_{\max}\frac{2\beta}{2\beta+\lambda} \tag{14}$$

Consequently:

$$\bar{p}^{r}_{\max} = \frac{p^{r}_{\max}\cdot h^2}{\eta\cdot U\cdot L_{tot}} = \frac{12\beta^2 N(H-1)(1-\Lambda)}{[H^3(\Lambda N+\beta-\Lambda)+N(1-\Lambda)+\frac{6\Lambda(N+\beta-\Lambda)}{6-5\Lambda}](N+\beta-0.5\Lambda)(2\beta+\Lambda)} \tag{15}$$

5. NUMERICAL SOLUTION

In order to find the pressure distribution, the finite difference method was used. The system of equations was solved using the Gauss-Seidel Method. If negative (sub-ambient) pressures are encountered, the pressures are set to zero in the iterative cycle, so the Reynolds continuity condition (the pressure gradient is zero along the normal of the cavitation zone) is obtained. The equations solved with the finite difference method are the Reynols equation, which for parallel surfaces is transformed into the Laplace equation, and the continuity of the flow in the discontinuity zones.

In order to verify the convergence of the solution, the number of meshing intervals was increased and it was found that the solution converged asymptotically to a certain value.

6. RESULTS

To find the optimal configuration of the slider, influence of the geometrical parameters of the textured slider is studied. The results obtained by analytical methods (continuous lines) are compared with the numerical values (represented by points). Because the numerical method takes into account the cavitation phenomenon, the method is compared with the analytical values $\bar{p}_{\max}$.

In figure 3 the influence of the number of dimples on one row N on the maximum dimensionless pressure is presented. The density of the dimples is ρ=0.64, the textured fraction is α=0,5 and the dimensionless film thickness is H=2. The dimensionless pressure decreases asymptotically with N. Above 25 cells per row the pressure decrease is low so N=25 seems to be o fair number for the next calculations.

In figure 4 the influence of the dimple density ρ on the maximum dimensionless pressure is presented (N=25, α=0.5, H=2). The dimensionless pressure increases linearly with the dimple density. By extrapolation the value of $\bar{p}$ at ρ=1 is 0.33, exactly the value of the dimensionless pressure for a stepped slider. This is explained by the fact that when the dimples occupy the entire surface, the slider becomes a stepped slider. It can be observed that the analytical solution results are the same as the numerical values at higher densities.

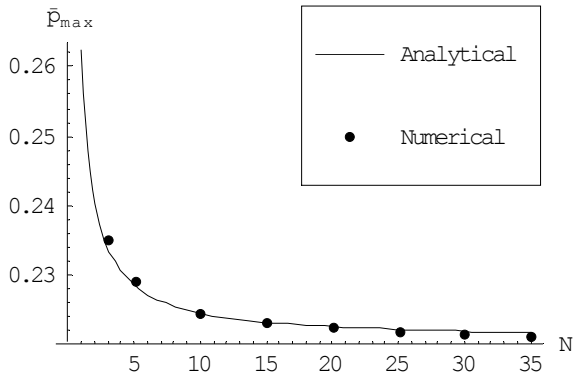

Figure 3: dimensionless pressure variation with N

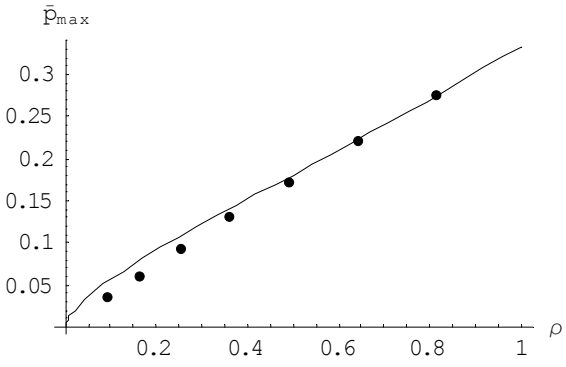

Figure 4: dimensionless pressure variation with ρ

The influence of the dimple depth *s* on the maximum dimensionless pressure is presented in figure 5, for three different densities: ρ=0.49, ρ=0.64, ρ=0.81 (N=25, α=0.5). The H value, which corresponds to a maximal pressure, is H=1.7, the same value as for a stepped bearing.

In figure 6 the influence of the textured fraction α on the maximum dimensionless pressure is presented (ρ=0.81, N=25, H=2). The α value which corresponds to a maximal pressure in α=0.7, the same value as for a stepped bearing.

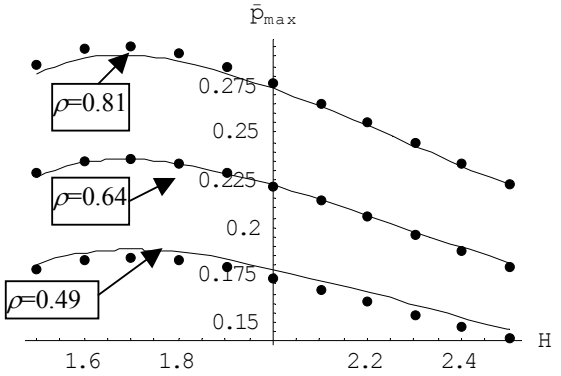

Figure 5: dimensionless pressure variation with H

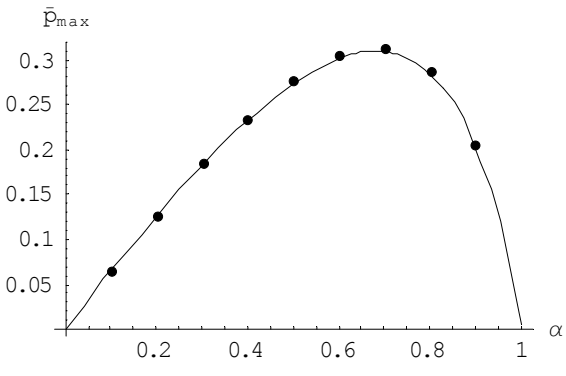

Figure 6: dimensionless pressure variation with α

7. CONCLUSIONS

From the results presented above, in order to maximize the load carrying capacity of the slider, an optimal configuration would be:

- The number of dimples on one row N>25
- The dimple density as large as possible. The maximal dimple density depends on the manufacturing technology adopted.
- The dimensionless film thickness H=1.7.

- The textured fraction α=0.7.

The partially textured slider presents lower load carrying capacity as a stepped slider, but can be more easily manufactured by various technologies (e.g. lithography).

8. ACKNOWLEDGEMENTS

The authors express their gratitude to Phd. st. Daniel Găman and Assoc. Prof. Traian Cicone for their precious help.

9. REFERENCES

[1] Brizmer V, Klingerman, Y, Etsion, I., ***A laser surface textured parallel thrust bearing***, Trybology Transactions, Vol 46, No 3, pp. 397-403, 2003

[2] Burstein, L., Ingman, D., ***Effect of pore ensemble statistics on load support of mechanical seals with pore-covered faces***, Journal of Tribology, Vol.121, pp.927-932, 1999

[3] Etsion, I., ***A laser surface textured hydrostatic mechanical seal***, Trybology Transactions,Vol 45,No 3,pp 430-434, 2002

[4] Etsion, I., Burstein, L, ***A model for mechanical seals with regular microsurface structure***, Tribology Transactions, Vol. 39, No. 3, pp. 677-683, 1996

[5] Etsion, I., Halperin, G., Brizmer, V., Kligerman, Y., ***Experimental investigation of laser surface textured parallel thrust bearings***, Tribology Letters, Vol.17, No.2, August 2004

[6] Etsion, I., Klingerman, Y., ***Analytical and experimental investigation of laser-textured mechanical seal faces***, Tribology Transactions, Vol 42, No. 3,pp. 511-516, 1999

[7] Golloch, R., Merker, G.P., Kessen, U., Brinkmann , S., ***Benefits of laser-structured cylinder liners for internal combustion engines***, 14th International Colloquium Tribology,Esslingen,Germany,Vol.1,pp.321-328, 2004

[8] Hamilton, D.B., Walowit, J.A., Allen, C.M., ***A Theory of Lubrication by Micro-irregularities***, ASME-ASLE Lubrication Conference, October 18-20 Paper No. 65-Lub-11, 1965

[9] Ronen, A., Etsion,I., Klingerman, Y., ***Friction-reducing surface-texturing in reciprocating automotive components***, Tribology Transactions, Vol. 44, No. 3,pp. 359-366, 2001

[10] Ryk, G, Klingerman, Y., Etsion, I., ***Experimental investigation of laser surface texturing for reciprocating automotive components***, Tribology Transactions, Vol. 45, No. 4, pp. 444-449, 2002